Computer Modeling in Engineering & Sciences
DOI:10.32604/cmes.2020.011871
Article

Tech Science Press

The Efficient Finite Element Methods for Time-Fractional Oldroyd-B Fluid Model Involving Two Caputo Derivatives

An Chen*

College of Science, Guilin University of Technology, Guilin, 541004, China
*Corresponding Author: An Chen. Email: chena@glut.edu.cn
Received: 02 June 2020; Accepted: 10 August 2020

Abstract: In this paper, we consider the numerical schemes for a time-fractional Oldroyd-B fluid model involving the Caputo derivative. We propose two efficient finite element methods by applying the convolution quadrature in time generated by the backward Euler and the second-order backward difference methods. Error estimates in terms of data regularity are established for both the semidiscrete and fully discrete schemes. Numerical examples for two-dimensional problems further confirm the robustness of the schemes with first- and second-order accurate in time.

Keywords: Oldroyd-B fluid model; caputo derivative; finite element method; convolution quadrature; error estimate; data regularity

1 Introduction

In this paper, we investigate efficient numerical schemes for the time-fractional Oldroyd-B fluid model involving the Caputo derivative in time. Let $\Omega \subset \mathbb{R}^n\,(n=1,2,3)$ be a bounded convex domain with a smooth boundary $\partial\Omega$, $T>0$ be a fixed time. The equation is stated as follows.

$$\left(\partial_t + a_1 {}_C D_{0,t}^{\alpha}\right) u(x,t) = \mu\left(1 + a_3 {}_C D_{0,t}^{\gamma}\right)\Delta u(x,t) + f(x,t), \quad \text{in} \quad \Omega\times(0,T) \tag{1}$$

with a homogeneous Dirichlet boundary condition $u(x,t)=0$ on $\partial\Omega\times(0,T]$ and the initial value conditions $u(x,0)=v(x)$ and $\partial_t u(x,0)=b(x)$. Here, the parameters μ, a_1 and a_3 are some fixed positive constants, the source term f and the initial value conditions v and b are given functions. The fractional orders $\gamma\in(0,1]$ and $\alpha\in(1,2]$. The fractional derivative ${}_C D_{0,t}^{\nu}$ with $\nu\in(n-1,n]$ is in Caputo sense defined by

$${}_C D_{0,t}^{\nu} u(\cdot,t) = {}_{RL} D_{0,t}^{-(n-\nu)} \frac{\partial^n}{\partial t^n} u(\cdot,t),$$

where the Riemann–Liouville (R–L) integral ${}_{RL} D_{0,t}^{-\nu}$ with $\nu>0$ is given by

$${}_{RL} D_{0,t}^{-\nu} u(\cdot,t) = \frac{1}{\Gamma(\nu)} \int_0^t (t-s)^{\nu-1} u(\cdot,s)\, ds.$$

Here $\frac{\partial^n}{\partial t^n}u(\cdot,t)$ is the n-th partial derivative of u with respect to t and $\Gamma(\cdot)$ is the Gamma function.

Over the last few decades, the studies of viscoelastic materials with fractional models have attracted many scholars' attention [1]. It seems that fractional models can provide another way to preserve the possibility for relatively simple description of the complex behavior of non-Newtonian viscoelastic fluids. The Oldroyd-B fluid can be regarded as one particular subclass of non-Newtonian fluids [2]. One can refer to [3–6] and the references therein for more details about the application. The reason why we prefer to consider the Caputo derivative rather than R–L derivative (see the next section for its definition) in the modeling of abnormal phenomenon in Oldroyd-B fluid is as follows. It is well known that the R–L derivative played an important role in the development of the theory of fractional calculus. However, it seems that the initial conditions for fractional models involving R–L derivative in time is not physically interpretable in applied problems, since they alway contain the limit values of the R–L derivative at $t=0$. So their solutions may be not practically useful due to the unknown physical interpretation for such kinds of initial conditions [7]. This motivates us to use the Caputo derivative instead of R–L derivative in the generalized Oldroyd-B fluid problem, which may lead to a more practical use. By using the method of separation of variables, the analytical solution of Eq. (1) can be derived and expressed in terms of the multivariate Mittag–Leffler function [8]. In this paper, we do not intend to go further for solution theory since it will be off the focus of the current paper. We leave the rigorous analysis of the regularity of the solution to be one of the future possible study.

The numerical schemes for the fractional model (1) or its variants (the Riemann–Liouville derivative version with zero a_1 or a_3) have been studied extensively in the literatures, [9,10], to name just a few. For more details, see the references therein. Bazhlekova et al. proposed two fully discrete schemes for the Rayleigh–Stokes problem for a generalized second-grade fluid, that is the case $a_1=0$ in Riemann–Liouville derivative version [9]. Their numerical schemes are based on the convolution quadrature in time generated by the backward Euler and the second-order backward difference methods. However they only investigated the error estimates for homogeneous problem with $f=0$. AI-Maskari et al. [10] further studied the finite element methods for time-fractional Oldroyd-B fluid problem with zero initial value condition b by convolution quadrature in time. They derived the optimal error estimates for smooth and nonsmooth data with $v\in\dot{H}^2(\Omega)$ and $v\in L^2(\Omega)$ (Section 2 for such definitions), respectively.

Numerical scheme for the case $a_3=0$ in Eq. (1) have been studied by some literatures [11–14]. Ren et al. [11] presented a compact alternating direction implicit (ADI) scheme for the two-dimensional time-fractional Cattaneo equation. Zhao et al. [12] proposed a compact Crank–Nicolson scheme and they also considered the two-dimensional case. Chen et al. [13] proposed an efficient ADI Galerkin method for time-fractional partial differential equation with damping. Recently, Li et al. introduced a high-order accurate numerical method for the time-fractional Cattaneo equation. Their numerical scheme is based on the Galkerin–Legendre spectral method in space and the Chebyshev collocation method in time [14]. It is worth noting that Ji et al. [15] proposed a new nanoscale heat transfer model based on the Caputo type fractional dual-phase-lagging heat conduction equation. Their model has the similar structure with the time-fractional Oldroyd-B fluid model, that is the case $\gamma=\alpha-1$ in Eq. (1). By using the L1 method in time, they developed a finite difference scheme for the time-fractional dual-phase-lagging model.

In order to obtain the desired convergence order, many efficient schemes often rely on some requisite regularity on the solution. Sometimes such assumption on the solution are too strong and make those numerical schemes less efficient or even useless in practical application.

In this paper, we aim to propose the robust and efficient numerical schemes for the fractional model (1) by applying the popular convolution quadrature method. The convolution quadrature method for solving fractional model has received considerable attenction [16,17]. The convolution quadrature method developed by Lubich [18] can provide a flexible framework for constructing some reliable numerical methods. So in this paper, we deduce two fully discrete schemes for (1) based on the linear finite element method in space and convolution quadrature in time generated by the backward Euler and the second-order backward difference methods. By the strategy developed in [19], we investigate the error estimates with respect to data regularity (Theorems 4.3 and 4.5).

We find that only smooth data of v fulfill the requirement for the second-order spatial accuracy of the proposed schemes, while the nonsmooth data (that is $v \in L^2(\Omega)$) would deteriorate the spatial accuracy. However, both smooth and nonsmooth data v can ensure the desired temporal convergence orders in the fully discrete schemes. We make some discussions on such situation (Remarks 4.1, 4.3, and 4.5) and numerically confirm our conclusions (Tabs. 7 and 8). To the best of our knowledge, it seems that such results have not been found in the existing literatures yet.

The rest of this paper is organized as follows. In Section 2, we introduce some preliminaries which are need in the numerical study. Two fully discrete schemes using the Galerkin finite element method in space and convolution quadrature in time are developed in Section 3. In Section 4, the error analysis of the schemes are investigated. In Section 5, numerical examples for two-dimensional problems are provided to support our theoretical results. The conclusions are presented in Section 6.

Throughout this paper, the notation c is denoted as a constant which may vary at different occurrences, but is always independent of the mesh size h and the time step size τ.

2 Preliminary

We first list some useful notations in this part.

(1) Some function spaces and the corresponding norms. Denote $(\cdot,\cdot)$ as the inner product on $L^2(\Omega)$ and the L^2-norm is $\|\cdot\|$. For $r \geq 0$, let $\dot{H}^r(\Omega)$ be the subspace of $L^2(\Omega)$ induced by the norm

$$\|v\|^2_{\dot{H}^r(\Omega)} = \|(-\Delta)^{r/2} v\|^2 = \sum_{j=1}^{\infty} \lambda_j^r \left(v, \phi_j\right)^2,$$

where $\{\lambda_j\}_{j=1}^{\infty}$ and $\{\phi_j\}_{j=1}^{\infty}$ are the Dirichlet eigenvalues and eigenfunctions of $-\Delta$, respectively. Here, $\{\phi_j\}_{j=1}^{\infty}$ is an orthonormal basis in $L^2(\Omega)$. Hence, $\|v\|_{\dot{H}^0(\Omega)} = \|v\|$ is the norm on $L^2(\Omega)$, $\|v\|_{\dot{H}^1(\Omega)} = \|\nabla v\|$ is also the norm on $H_0^1(\Omega)$, and $\|v\|_{\dot{H}^2(\Omega)} = \|Av\|$ is the equivalent norm in $H^2(\Omega) \cap H_0^1(\Omega)$ [20].

(2) Laplace transform and a related property. The Laplace transform of f with respect to t is denoted as

$$\hat{f}(z) = \mathcal{L}\{f(t); z\} := \int_0^\infty e^{-zt} f(t)\, dt.$$

One can readily derive that

$$\mathrm{L}\left\{ {}_C D_{0,t}^{\nu} f(t); z \right\} = z^{\nu} \hat{f}(z) - \sum_{k=0}^{n-1} z^{\nu-k-1} f^{(k)}(0),$$

with $n-1 < \nu \leq n$.

(3) Riemann–Liouville derivative and its relationship with Caputo derivative. For $n-1 < \nu < n$, The definition of R–L derivative is given by

$${}_{RL} D_{0,t}^{\nu} \varphi(t) = \frac{\partial^n}{\partial t^n} {}_{RL} D_{0,t}^{-(n-\nu)} \varphi(t).$$

The relationships between Caputo and R–L derivatives are as follows.

$${}_C D_{0,t}^{\gamma} \varphi(t) = {}_{RL} D_{0,t}^{\gamma} (\varphi(t) - \varphi(0)),$$

and

$${}_C D_{0,t}^{\alpha} \varphi(t) = {}_{RL} D_{0,t}^{\alpha} \big(\varphi(t) - \varphi(0) - t\varphi'(0)\big),$$

(4) The resolvent estimate. It is known that the operator $A := -\Delta$ is selfadjoint and positive definite, so the resolvent estimate

$$\| \left(z^{\gamma} I + A\right)^{-1} \| \leq M |z|^{-\gamma}, \quad \forall z \in \Sigma_\theta, \tag{2}$$

holds [20]. Here, the sector $\Sigma_\theta = \{z \in \mathbb{C}, z \neq 0, |\arg z| < \theta\}$ with $\theta \in (\pi/2, \pi)$ and M depends on θ. The notation $\|\cdot\|$ denotes the operator norm from $L^2(\Omega) \to L^2(\Omega)$, which has the same form with the L^2-norm.

We also need the notations from the operational calculus [21].

Let $K(z)$ be a complex valued or operator valued function that is analytic in a sector Σ_θ where $\theta \in \left(\frac{\pi}{2}, \pi\right)$. Besides, the function $K(z)$ is bounded by

$$\|K(z)\| \leq M\ |z|^{-\lambda}, \quad \forall z \in \Sigma_\theta, \tag{3}$$

for some real numbers λ and M. Then $K(z)$ is the Laplace transform of a distribution k on the real line, which vanishes for $t < 0$, has its singular support empty or concentrated at $t = 0$, and which is an analytic function for $t > 0$ ([18,21] for more details). By the inversion Laplace transform for $K(z)$ with $t > 0$, we get

$$k(t) = \frac{1}{2\pi \mathrm{i}} \int_\Gamma K(z)\, e^{zt} dz, \quad t > 0. \tag{4}$$

Here the contour Γ lies in Σ_θ, and parallel to its boundary and oriented with increasing imaginary part. We denote that $\Gamma_{\theta,\delta} = \{z \in \mathbb{C}: |z| = \delta, |\arg z| \leq \theta\} \cup \left\{z \in \mathbb{C}: z = \rho e^{\pm i\theta}, \rho \geq \delta\right\}$.

We define $K(\partial_t)$ as the operator of convolution with the kernel k: $K(\partial_t)g = k * g$. Here ∂_t is the time differentiation and g is suitably smooth. We divide the time interval $[0, T]$ into a uniform grid with a grid point $t_k = k\tau$. Here the time step size $\tau = T/N$ with a positive integer N. The convolution quadrature $K(\partial_\tau)g$ of $K(\partial_t)g$ at $t = t_n$ is given by

$$K(\partial_\tau) g(t_n) = \sum_{k=0}^{n} \omega_k(\tau) g\left(t_{n-k}\right), \tag{5}$$

where the quadrature weights $\omega_k(\tau)$ are determined by the generating function

$$\sum_{k=0}^{\infty} \omega_k(\tau) \zeta^k = K\left(\frac{\vartheta(\zeta)}{\tau}\right). \tag{6}$$

Here ϑ is the quotient of the generating polynomials of linear multistep method [18]. In this paper, we focus on the backward Euler (BE) and the second-order backward difference (SBD) methods, for which $\vartheta(\zeta) = 1 - \zeta$ and $\vartheta(\zeta) = (1-\zeta) + (1-\zeta)^2/2$, respectively.

The convolution quadrature has the following error estimates [22].

Lemma 2.1. Let $K(z)$ be analytic in Σ_θ and (3) hold. Then for $g(t) = ct^{\sigma-1}$, the convolution quadrature based on BE ($p = 1$) or SBD ($p = 2$) satisfies

$$\| (K(\partial_t) - K(\partial_\tau)) g(t) \| \leq \begin{cases} ct^{\lambda-1}\tau^\sigma, & 0 < \sigma \leq p, \\ ct^{\lambda-1+\sigma-p}\tau^p, & \sigma \geq p. \end{cases}$$

Finally, we state some basic properties for the functions

$$h(z) = 1/\left(z + a_1 z^\alpha\right) \quad \text{and} \quad g(z) = \left(z + a_1 z^\alpha\right)/\left(\mu\left(1 + a_3 z^\gamma\right)\right) \tag{7}$$

with $z \in \Sigma_\theta$ by the following lemma.

Lemma 2.2. Let $\theta \in (\pi/2, \pi/\alpha)$ be fixed. Then, for any $z \in \Sigma_\theta$, we have $g(z) \in \Sigma_{\overline{\theta}}$, where $\overline{\theta} = \alpha\theta < \pi$,

$$|g(z)| \leq c\frac{1}{\mu}\left(|z| + a_1|z|^\alpha\right) \min\left\{1, \frac{1}{a_3}|z|^{-\gamma}\right\},$$

and

$$|h(z)| \leq c \min\left\{|z|^{-1}, \frac{1}{a_1}|z|^{-\alpha}\right\}.$$

Proof. The property of $g(z)$ has been provided in [10]. The bound $|h(z)|$ can be derived in a similar way with $|g(z)|$, the proof is thus completed.

3 Fully Discrete Schemes

In this section, we propose two fully discrete finite element methods by using the standard Galerkin finite element method in space and convolution quadrature in time.

3.1 Semidiscrete Galerkin Scheme in Space

A partition of the domain Ω is denoted by $\mathcal{T}_h$ in which h is the maximal length of the sides of the triangulation $\mathcal{T}_h$. Then the continuous piecewise linear finite element space V_h is given by

$$V_h = \left\{ v_h \in H_0^1(\Omega) : v_{h|T} \text{ is a linear function and } \quad \forall T \in \mathcal{T}_h \right\}.$$

The $L^2(\Omega)$ orthogonal projection $P_h : L^2(\Omega) \to V_h$ is defined by

$$(P_h\varphi, \chi) = (\varphi, \chi), \quad \forall \chi \in V_h,$$

and the Ritz projection $R_h : H_0^1(\Omega) \to V_h$ is defined by

$$(R_h\varphi, \chi) = (\nabla\varphi, \nabla\chi), \quad \forall \chi \in V_h.$$

From the definitions of P_h and R_h, one can see that they are stable in L^2 and H_0^1, respectively. We remark that these properties would be used frequently and may not be mentioned explicitly in the error estimates. We also need the following approximation properties of these two operators P_h and R_h, one may also refer to Theorem 1.1 and Lemma 1.1 in the book [20].

Lemma 3.1. The following approximation properties of the operators P_h and R_h hold:

$$\|P_h\varphi - \varphi\| + h\|\nabla(P_h\varphi - \varphi)\| \le ch^2\|\varphi\|_{\dot{H}^2(\Omega)}, \quad \forall \varphi \in \dot{H}^2(\Omega),$$

$$\|R_h\varphi - \varphi\| + h\|\nabla(R_h\varphi - \varphi)\| \le ch^2\|\varphi\|_{\dot{H}^2(\Omega)}, \quad \forall \varphi \in \dot{H}^2(\Omega).$$

The semidiscrete Galerkin scheme for (1) reads: Find $u_h(t) = u_h(\cdot, t) \in V_h$ such that

$$\left(\left(\partial_t + a_{1C}D_{0,t}^{\alpha}\right)u_h, \chi\right) + \mu\left(1 + a_{3C}D_{0,t}^{\gamma}\right)a\left(u_h, \chi\right) = \left(f, \chi\right), \quad \forall \chi \in V_h, \tag{8}$$

with the initial value conditions $u_h(0) = v_h \in V_h$ and $\partial_t u_h(0) = b_h \in V_h$. Here v_h and b_h are proper approximations to the functions v and b, respectively. The bilinear form $a(u, v)$ is given by $(\nabla u_h, \nabla\chi)$.

By introducing the discrete Laplacian $\Delta_h : V_h \to V_h$ with the definition:

$$-(\Delta_h\varphi, \chi) = (\nabla\varphi, \nabla\chi), \quad \forall\varphi, \quad \chi \in V_h,$$

and letting $A_h = -\Delta_h$, we can rewrite the semidiscrete scheme (8) as follows.

$$\left(\partial_t + a_{1C}D_{0,t}^{\alpha}\right)u_h(t) + \mu\left(1 + a_{3C}D_{0,t}^{\gamma}\right)A_h u_h(t) = f_h(t), \quad t > 0, \tag{9}$$

where $f_h(t) = P_h f(t)$.

3.2 Fully Discrete Schemes with Convolution Quadrature in Time

In this part we apply convolution quadrature based on BE and SBD formulas in time to obtain two fully discrete schemes.

Using the relationship between Caputo and R–L derivatives, we derive from the semidiscrete scheme (9) that

$$\partial_t u_h(t) + a_{1RL}D_{0,t}^{\alpha}(u_h(t) - v_h - tb_h) + \mu A_h u_h(t) + \mu a_{3RL}D_{0,t}^{\gamma}A_h(u_h(t) - v_h) = f_h(t),$$

that is

$$\left(\partial_t + a_{1RL}D_{0,t}^{\alpha}\right)u_h(t) + \mu\left(1 + a_{3RL}D_{0,t}^{\gamma}\right)A_h u_h(t) = a_{1RL}D_{0,t}^{\alpha}(v_h + tb_h) + \mu a_{3RL}D_{0,t}^{\gamma}A_h v_h + f_h(t). \tag{10}$$

Applying $K(\partial_t)=\left(\partial_t+a_{1RL}D^{\alpha}_{0,t}+\mu\left(1+a_{3RL}D^{\gamma}_{0,t}\right)A_h\right)^{-1}$ on both sides of the semidiscrete scheme (10), we obtain

$$u_h(t)=K(\partial_t)\left(a_{1RL}D^{\alpha}_{0,t}(v_h+tb_h)+\mu a_{3RL}D^{\gamma}_{0,t}A_hv_h+f_h(t)\right), \tag{11}$$

with $t>0$. Combining the convolution quadrature with the associativity of convolution, we have the approximation of $u_h(t_n)$ at $t_n=n\tau$ with U_h^n by

$$U_h^n=K(\partial_\tau)\left(a_1\partial_\tau^{\alpha}(v_h+tb_h)+\mu a_3\partial_\tau^{\gamma}A_hv_h+F_h^n\right), \tag{12}$$

where $n=1,2,\ldots,N$, $U_h^0=v_h$, and $F_h^n=P_hf(t_n)$. Here $K(\partial_\tau),\partial_\tau^{\alpha}$, and ∂_τ^{γ} are the convolution quadratures with $\vartheta(\zeta)=1-\zeta$ for BE scheme, or $\vartheta(\zeta)=\frac{3}{2}-2\zeta+\frac{1}{2}\zeta^2$ for SBD scheme.

Thus, the BE scheme for (12) is stated as: Find U_h^n for $n\geq 1$ such that

$$\left(\partial_\tau+a_1\partial_\tau^{\alpha}\right)U_h^n+\mu\left(1+a_3\partial_\tau^{\gamma}\right)A_hU_h^n=a_1\partial_\tau^{\alpha}(v_h+tb_h)+\mu a_3\partial_\tau^{\gamma}A_hv_h+F_h^n. \tag{13}$$

Remark 3.1. Actually, the term $\partial_\tau^{\alpha}tb_h$ in Eq. (13) may also be replaced with the exact expression ${}_{RL}D^{\alpha}_{0,t}tb_h$, that is ${}_{RL}D^{\alpha}_{0,t}tb_h=t^{1-\alpha}b_h/\Gamma(2-\alpha)$.

Next, we present a robust numerical scheme which can maintain the second-order accuracy for the scheme (12). Since

$$K(\partial_t)=\left(a_{1RL}D^{\alpha}_{0,t}+\mu a_{3RL}D^{\gamma}_{0,t}A_h\right)^{-1}-K(\partial_t)\left(a_{1RL}D^{\alpha}_{0,t}+\mu a_{3RL}D^{\gamma}_{0,t}A_h\right)^{-1}(\partial_t+\mu A_h),$$

the semidiscrete scheme (11) can be rewritten as

$$u_h(t)=v_h+K(\partial_t)\left(-\left(\partial_t+\partial_{tRL}D^{-1}_{0,t}(\mu A_h)\right)v_h+a_{1RL}D^{\alpha}_{0,t}tb_h+\partial_{tRL}D^{-1}_{0,t}f_h(0)+\tilde{f}_h(t)\right), \tag{14}$$

where $t>0$ and $\tilde{f}_h(t)=f_h(t)-f_h(0)$. By noting that $-\partial_tv_h=0$, one has

$$U_h^n=v_h+K(\partial_\tau)\left(-\partial_{\tau RL}D^{-1}_{0,t}(\mu A_h)v_h+a_1\partial_\tau^{\alpha}tb_h+\partial_{\tau RL}D^{-1}_{0,t}f_h(0)+\tilde{F}_h^n\right). \tag{15}$$

Letting $1_\tau=(0,3/2,1,1,\ldots)$, and noting $1_\tau=\partial_{\tau RL}D^{-1}_{0,t}$, we obtain the SBD scheme as follows: Find U_h^n for $n\geq 1$ such that

$$\left(\partial_\tau+a_1\partial_\tau^{\alpha}+\mu\left(1+a_3\partial_\tau^{\gamma}\right)A_h\right)\left(U_h^n-v_h\right)=-1_\tau(\mu A_h)v_h+a_1\partial_\tau^{\alpha}tb_h+1_\tau f_h(0)+\tilde{F}_h^n. \tag{16}$$

that is,

$$\partial_\tau U_h^n+a_1\partial_\tau^{\alpha}U_h^n+\mu\left(1+a_3\partial_\tau^{\gamma}\right)A_hU_h^n=\partial_\tau U_h^0+a_1\partial_\tau^{\alpha}U_h^0+\mu a_3\partial_\tau^{\gamma}A_hU_h^0+a_1\partial_\tau^{\alpha}tb_h+\bar{F}_h^n,$$

with $\overline{F}_h^n=F_h^1-\frac{1}{2}(\mu A_h)U_h^0+\frac{1}{2}F_h^0$ when $n=1$, and $\bar{F}_h^n=F_h^n$ for $n\geq 2$.

4 Error Estimates

In this section, we derive the error estimates for the proposed numerical schemes by using the strategy developed in [19] which is originated in [21]. For the convenience of discussion, we always assume $a_1=1$ when necessary.

4.1 Error Estimates for the Semidiscrete Scheme

We first consider the homogeneous problem with $f=0$ and derive the corresponding integral representation of the solution.

An application of the Laplace transform to (1) yields

$$z\hat{u}(z)-v+a_1\left(z^{\alpha}\hat{u}(z)-z^{\alpha-1}v-z^{\alpha-2}b\right)+\mu A\left(\hat{u}(z)+a_3\left(z^{\gamma}\hat{u}(z)-z^{\gamma-1}v\right)\right)=0.$$

So,

$$\hat{u}(z)=\hat{E}(z)\left(\left(1+a_1z^{\alpha-1}+\mu a_3Az^{\gamma-1}\right)v+a_1z^{\alpha-2}b\right), \tag{17}$$

where

$$\hat{E}(z)=h(z)\,g(z)\,(g(z)\,I+A)^{-1},$$

and the functions $h(z)$ and $g(z)$ are given by Eq. (7).

So the solution $u(t)$ can be represented by

$$u(t)=\frac{1}{2\pi i}\int_{\Gamma_{\theta,\delta}}e^{zt}\hat{E}(z)\left(\left(1+a_1z^{\alpha-1}+\mu a_3Az^{\gamma-1}\right)v+a_1z^{\alpha-2}b\right)dz. \tag{18}$$

Similarly, the solution $u_h(t)$ to Eq. (9) can be represented by the following:

$$u_h(t)=\frac{1}{2\pi i}\int_{\Gamma_{\theta,\delta}}e^{zt}\hat{E}_h(z)\left(\left(1+a_1z^{\alpha-1}+\mu a_3A_hz^{\gamma-1}\right)v_h+a_1z^{\alpha-2}b_h\right)dz, \tag{19}$$

where

$$\hat{E}_h(z)=h(z)\,g(z)\,(g(z)\,I+A_h)^{-1}.$$

From the structures of $\hat{E}(z)$ and $\hat{E}_h(z)$, we let $F_h(z)=(g(z)I+A)^{-1}-(g(z)I+A_h)^{-1}P_h$ for notation conveience. The operator $F_h(z)$ has the following property which plays a key role in the error estimate [9].

Lemma 4.1. The following estimate holds:

$$\|F_h(z)\,\varphi\|+h\|\nabla F_h(z)\,\varphi\|\le ch^2\|\varphi\|.$$

Now we are ready to present the error estimates for the semidiscrete problem.

Theorem 4.1. Let u be the solution of problem (1) with $v\in\dot{H}^2(\Omega)$ and $f=0$, and set u_h be the solution of Eq. (9) with $v_h=R_hv$. Then, the following estimates hold:

(a) If $b\in\dot{H}^2(\Omega)$ and $b_h=R_hb$, then

$$\|e_h(t)\|+h\|\nabla e_h(t)\|\le ch^2\left(\left(t^{\alpha-1}+1\right)\|v\|_{\dot{H}^2(\Omega)}+t\|b\|_{\dot{H}^2(\Omega)}\right).$$

(b) If $b\in L^2(\Omega)$ and $b_h=P_hb$, then

$$\|e_h(t)\|+h\|\nabla e_h(t)\|\le ch^2\left(\left(t^{\alpha-1}+1\right)\|v\|_{\dot{H}^2(\Omega)}+t^{\gamma-\alpha+1}\|b\|\right).$$

Proof. For $v, b \in \dot{H}^2(\Omega)$, the error $e_h(t) := u(t) - u_h(t)$ can be represented by

$$\begin{aligned} e_h(t) = & \frac{1}{2\pi i} \int_{\Gamma_{\theta,\delta}} e^{zt} \left(1 + a_1 z^{\alpha-1}\right) \left(\hat{E}(z) - \hat{E}_h(z) R_h\right) v dz \\ & + \frac{1}{2\pi i} \int_{\Gamma_{\theta,\delta}} e^{zt} \left(\mu a_3 z^{\gamma-1}\right) \left(\hat{E}(z) A - \hat{E}_h(z) A_h R_h\right) v dz \\ & + \frac{1}{2\pi i} \int_{\Gamma_{\theta,\delta}} e^{zt} a_1 z^{\alpha-2} \left(\hat{E}(z) - \hat{E}_h(z) R_h\right) b \Big) dz =: I + II + III. \end{aligned} \tag{20}$$

For the first term I, by the identity

$$h(z) g(z) (g(z) I + A)^{-1} = h(z) I - h(z) (g(z) I + A)^{-1} A,$$

and noting that $A_h R_h = P_h A$, we can obtain

$$I = \frac{1}{2\pi i} \left(\int_{\Gamma_{\theta,\delta}} e^{zt} \left(1 + a_1 z^{\alpha-1}\right) (-h(z)) F_h(z) A v dz + \int_{\Gamma_{\theta,\delta}} e^{zt} \left(1 + a_1 z^{\alpha-1}\right) h(z) (v - R_h v) dz \right).$$

By Lemmas 3.1 and 4.1, we obtain

$$\begin{aligned} \|I\| & \le c h^2 \|v\|_{\dot{H}^2(\Omega)} \int_{\Gamma_{\theta,1/t}} e^{Re(z)t} |h(z)| \left(1 + a_1 |z|^{\alpha-1}\right) |dz| \\ & \le c h^2 \|v\|_{\dot{H}^2(\Omega)} \int_{\Gamma_{\theta,1/t}} e^{Re(z)t} \min\left\{ |z|^{-1}, \frac{1}{a_1} |z|^{-\alpha} \right\} \left(1 + a_1 |z|^{\alpha-1}\right) |dz| \\ & \le c h^2 \|v\|_{\dot{H}^2(\Omega)} \min\left\{ 1, \frac{1}{a_1} t^{\alpha-1} \right\} \left(1 + a_1 t^{-\alpha+1}\right) \\ & \le c \left(t^{\alpha-1} + 1\right) h^2 \|v\|_{\dot{H}^2(\Omega)}. \end{aligned}$$

Note that the last two terms II and III can be recast as

$$II = \frac{1}{2\pi i} \int_{\Gamma_{\theta,\delta}} e^{zt} \left(\mu a_3 z^{\gamma-1}\right) h(z) g(z) F_h(z) A v dz,$$

$$III = \frac{1}{2\pi i} \int_{\Gamma_{\theta,\delta}} e^{zt} a_1 z^{\alpha-2} h(z) \left(-F_h(z) A b + (b - R_h b)\right) dz.$$

Thus, for the second term II, by Lemma 4.1, we have

$$\begin{aligned} \|II\| & \le c h^2 \|v\|_{\dot{H}^2(\Omega)} \int_{\Gamma_{\theta,1/t}} e^{Re(z)t} \left(\mu a_3 |z|^{\gamma-1}\right) |h(z) g(z)| |dz| \\ & \le c h^2 \|v\|_{\dot{H}^2(\Omega)} \int_{\Gamma_{\theta,1/t}} e^{Re(z)t} \left(a_3 |z|^{\gamma-1}\right) \min\left\{ 1, \frac{1}{a_3} |z|^{-\gamma} \right\} |dz| \\ & \le c h^2 \|v\|_{\dot{H}^2(\Omega)} \left(a_3 t^{-\gamma+1}\right) \min\left\{ t^{-1}, \frac{1}{a_3} t^{\gamma-1} \right\} \le c h^2 \|v\|_{\dot{H}^2(\Omega)}. \end{aligned}$$

For the last term *III*, a use of Lemma 4.1 again yields

$$\begin{aligned}\|III\| &\le ch^2\|b\|_{\dot{H}^2(\Omega)}\int_{\Gamma_{\theta,1/t}} e^{Re(z)t}a_1|z|^{\alpha-2}|h(z)||dz| \\ &\le ch^2\|b\|_{\dot{H}^2(\Omega)}a_1 t^{-\alpha+2}\min\left\{1, t^{\alpha-1}\right\} \le ch^2 t\|b\|_{\dot{H}^2(\Omega)}.\end{aligned}$$

Putting the bounds of *I*, *II*, and *III* together, we complete the proof for the case (a) with L^2-estimates.

For the second case $b \in L^2(\Omega)$, by the error estimates in Eq. (20) for the first case (a), one just need to bound the third term *III* in Eq. (20) with P_h replacing R_h. By Lemma 4.1, we derive that

$$\begin{aligned}\|III\| \le& ch^2\|v\|\int_{\Gamma_{\theta,1/t}} e^{Re(z)t}\left(a_1|z|^{\alpha-2}\right)|h(z)g(z)||dz| \\ \le& ch^2\|v\|\int_{\Gamma_{\theta,1/t}} e^{Re(z)t}\left(a_1|z|^{\alpha-2}\right)\min\left\{1, \frac{1}{a_3}|z|^{-\gamma}\right\}|dz| \\ \le& ch^2\|v\|\left(a_1 t^{-\alpha+2}\right)\min\left\{t^{-1}, \frac{1}{a_3}t^{\gamma-1}\right\} \le ct^{\gamma-\alpha+1}h^2\|v\|.\end{aligned}$$

So the L^2-estimates are proved completed. A similar argument yields the H^1-estimates for both cases (a) and (b).

Remark 4.1. The result in Theorem 4.1 may not be improved to the case: $v, b \in L^2(\Omega)$. As a matter of fact, by the error representation in Eq. (20) (let $v_h = P_h v$), one may derive that

$$\begin{aligned}\|II\| \le& \left\|\frac{1}{2\pi i}\left(\int_{\Gamma_{\theta,\delta}} e^{zt}\left(\mu a_3 z^{\gamma-1}\right)h(z)g(z)\left((v-v_h)+(-g(z)F_h(z)v)\right)dz\right)\right\| \\ \le& c\|v-v_h\|\int_{\Gamma_{\theta,1/t}} e^{Re(z)t}\left(\mu a_3|z|^{\gamma-1}\right)|h(z)g(z)||dz| \\ &+ ch^2\|v\|\int_{\Gamma_{\theta,1/t}} e^{Re(z)t}\left(\mu a_3|z|^{\gamma-1}\right)|h(z)g(z)||g(z)||dz|.\end{aligned}$$

By Lemma 3.1, we conclude that the above error estimate is not $O(h^2)$ for the case $v \in L^2(\Omega)$ due to the appearance of the term $\|v-v_h\|$.

Now we consider the inhomogeneous problem with $f \neq 0$. By applying the Laplace transform, the solution $u(t)$ can be represented by

$$u(t) = \int_0^t G(t-s)f(s)\,ds, \tag{21}$$

where

$$G(t) = \frac{1}{2\pi i}\int_{\Gamma_{\theta,\delta}} e^{zt}\hat{E}(z)\,dz.$$

By a similar argument, the solution $u_h(t)$ to Eq. (9) is represented by

$$u_h(t) = \int_0^t G_h(t-s) P_h f(s)\, ds, \tag{22}$$

where

$$G_h(t) = \frac{1}{2\pi i} \int_{\Gamma_{\theta,\delta}} e^{zt} \hat{E}_h(z)\, dz.$$

Subtracting Eq. (21) from Eq. (22), we get

$$e_h(t) := u_h(t) - u(t) = \int_0^t (G_h(t-s) P_h - G(t-s)) f(s)\, ds = \int_0^t \tilde{G}_h(t-s) f(s)\, ds. \tag{23}$$

The operator $\tilde{G}_h$ has the following error estimate.

Lemma 4.2. Let $\phi \in L^2(\Omega)$, then there holds

$$\|\tilde{G}_h(t)\| + h\|\nabla \tilde{G}_h(t)\| \le ch^2 t^{\gamma-1}.$$

Proof. By Lemma 4.1, we readily obtain

$$\begin{aligned}\|\tilde{G}_h(t)\| &= \left\| \frac{1}{2\pi i} \int_{\Gamma_{\theta,\delta}} e^{zt} \left(\hat{E}_h(z) P_h - \hat{E}(z) \right) dz \right\| \\ &\le ch^2 \int_{\Gamma_{\theta,1/t}} e^{Re(z)t} |h(z)\, g(z)| \cdot |dz| \le ch^2 t^{\gamma-1}.\end{aligned}$$

A similar argument also yields

$$h\|\nabla \tilde{G}_h(t)\| \le ch^2 t^{\gamma-1}.$$

The proof is thus completed.

We are in position to state the error estimate for the inhomogeneous problem.

Theorem 4.2. Let u and u_h be the solutions of problems (1) with $f \in L^p(0,T;\Omega)$ and $v = b = 0$, and (9) with $v_h = b_h = 0$ and $f_h = P_h f$, respectively. Then, for $t > 0$,

$$\|e_h(t)\| + h\|\nabla e_h(t)\| \le ch^2 t^{\gamma-1/p} \|f\|_{L^p(0,T;L^2(\Omega))}.$$

Proof. Using Lemma 4.2 and Hölder's inequality for the error $e_h(t)$ in Eq. (23), we can readily derive the desired result. One may refer to Theorem 3.4 in [10] for similar discussions. Thus the proof is completed.

4.2 Error Estimates for the Fully Discrete Schemes

In this part, we derive the L^2-error estimates for the fully discrete schemes (13) and (16).

4.2.1 Error Estimates for the BE Method

We first consider the homogeneous problem with $f=0$.

Since the spatial error $u(t)-u_h(t)$ has been discussed in the previous part, we focus on the temporal error $u_h(t_n)-U_h^n$. We state the error estimates as below.

Lemma 4.3. Let u_h and U_h^n be the solutions of Eq. (9) and Eq. (13), respectively. Particularly, $v\in\dot{H}^2(\Omega)$, $f=0$, and $v_h=R_hv$. Then the following error estimates hold:

(a) If $b\in\dot{H}^2(\Omega)$ and $b_h=R_hb$, then

$$\|u_h(t_n)-U_h^n\|\le c\tau\left(\left(t_n^{-1}+a_3t_n^{\alpha-\gamma-1}\right)\|v\|_{\dot{H}^2(\Omega)}+\|b\|_{\dot{H}^2(\Omega)}\right).$$

(b) If $b\in L^2(\Omega)$ and $b_h=P_hb$, then

$$\|u_h(t_n)-U_h^n\|\le c\tau\left(\left(t_n^{-1}+a_3t_n^{\alpha-\gamma-1}\right)\|v\|_{\dot{H}^2(\Omega)}+\|b\|\right).$$

Proof. By Eqs. (11) and (12), we have

$$u_h(t_n)-U_h^n=\left(F_1(\partial_t)-F_1(\partial_\tau)\right)v_h+\left(F_2(\partial_t)-F_2(\partial_\tau)\right)tb_h=I+II,$$

where

$$F_1(z)=\hat{E}_h(z)\left(a_1z^\alpha+\mu a_3z^\gamma A_h\right) \tag{24}$$

and $F_2(z)=\hat{E}_h(z)(a_1z^\alpha)$.

Recall that $\hat{E}_h(z)=h(z)g(z)\left(g(z)I+A_h\right)^{-1}$, then we have

$$\|F_1(z)\|\le c\left(|z|^\alpha+\mu a_3|z|^\gamma A_h\right)\min\left\{|z|^{-1},|z|^{-\alpha}\right\},$$

and

$$\|F_2(z)\|\le c|z|^\alpha\min\left\{|z|^{-1},|z|^{-\alpha}\right\}.$$

So it follows from Lemma 2.1 (with $\sigma=1,p=1$, and the suitable chosen parameters λ) that

$$\begin{aligned}\|I\|&\le c\tau\left(\min\left\{t_n^{-\alpha},t_n^{-1}\right\}\|R_hv\|+\mu a_3\min\left\{t_n^{-\gamma},t_n^{\alpha-\gamma-1}\right\}\|A_hR_hv\|\right)\\&\le c\tau\left(t_n^{-1}\|R_hv\|+a_3t_n^{\alpha-\gamma-1}\|Av\|\right)\le c\tau\left(t_n^{-1}+a_3t_n^{\alpha-\gamma-1}\right)\|Av\|,\end{aligned}$$

where the estimate for the term R_hv in the last inequality has used the following two facts: $H_0^1(\Omega)$-stability of R_h and the equivalence between $\|\nabla v\|$ and $\|v\|_1$ in $H_0^1(\Omega)$.

For $b\in L^2(\Omega)$ and $b_h=P_hb$, by the bound of $\|F_2(z)\|$ and Lemma 2.1 (with $\sigma=2,p=1$, and some suitable parameters λ), the second term II can be derived that

$$\|II\|\le\|\left(F_2(\partial_t)-F_2(\partial_\tau)\right)t\|\|b_h\|\le c\tau\min\left\{t_n^{1-\alpha},1\right\}\|b\|\le c\tau\|b\|.$$

This together the bound $\|I\|$ yields the case (b). The case (a) can be derived similarly, so the proof is completed.

Remark 4.2. When proving the error estimate in terms of smooth data in $\dot{H}^2(\Omega)$, we only can obtain the terms with $\|v_h\|$ and $\|b_h\|$ instead of those with $\|A_hv_h\|$ and $\|A_hb_h\|$, and then

bound them by $\|Av\|$ and $\|Ab\|$ in view of $v_h = R_h v$ and $b_h = R_h b$. One may wonder whether this result can be improved to $\|A_h v_h\|$ and $\|A_h b_h\|$ where we can naturally have $\|Av\|$ and $\|Ab\|$ by using the identity $A_h R_h = P_h A$ and the L^2-stability of P_h. We find that such situation may not happen unless the term $\partial_t u$ in Eq. (1) vanishes.

Remark 4.3. By the equality

$$\hat{E}_h(z) A_h = h(z) g(z) (g(z) I + A_h)^{-1} A_h = h(z) g(z) \left(I - g(z) (g(z) I + A_h)^{-1} \right),$$

one can improve the above result with respect to the initial data $v \in L^2(\Omega)$ and $v_h = P_h v$, that is

$$\| U_h^n - u_h(t_n) \| \le c\tau \left(t_n^{-1} \|v\| + \|b\| \right).$$

Indeed, one may consider the term $\mu a_3 \hat{E}_h(z) z^\gamma A_h =: F_{12}(z)$ in Eq. (24). By noting that

$$\|F_{12}(z)\| \le c|z|^\gamma |h(z) g(z)| \le c|z|^\gamma \min\left\{1, \frac{1}{a_3}|z|^{-\gamma}\right\}, \quad \forall z \in \Sigma_\theta,$$

a use of Lemma 2.1 (with $\sigma = 1, p = 1$, and the suitable chosen parameters λ) yields

$$\| (F_{12}(\partial_t) - F_{12}(\partial_\tau)) v_h \| \le c\tau \min\left\{ t_n^{-\gamma-1}, \frac{1}{a_3} t_n^{-1} \right\} \|v\| \le c\tau t_n^{-1} \|v\|.$$

In view of Lemma 4.3, we readily obtain the desired results.

We now summarize the results for the error estimates of the fully discrete BE scheme (13) in the next theorem.

Theorem 4.3. Let u and U_h^n be the solutions of (1) and (13), respectively. Particularly, $v \in \dot{H}^2(\Omega), f = 0$, and $v_h = R_h v$. Then the following error estimates hold:

(a) If $b \in \dot{H}^2(\Omega)$ and $b_h = R_h b$, then

$$\| U_h^n - u(t_n) \| \le c \left(\left(\left(t_n^{-1} + a_3 t_n^{\alpha-\gamma-1} \right) \tau + h^2 \right) \|v\|_{\dot{H}^2(\Omega)} + \left(\tau + h^2 \right) \|b\|_{\dot{H}^2(\Omega)} \right).$$

(b) If $b \in L^2(\Omega)$ and $b_h = P_h b$, then

$$\| U_h^n - u(t_n) \| \le c \left(\left(\left(t_n^{-1} + a_3 t_n^{\alpha-\gamma-1} \right) \tau + h^2 \right) \|v\|_{\dot{H}^2(\Omega)} + \left(\tau + h^2 t_n^{\gamma-\alpha+1} \right) \|b\| \right).$$

Next we state the error estimates for the inhomogeneous problem with $f \neq 0$ but $v = b = 0$.

Theorem 4.4. Let u be the solution of the problem (1) with $v = b = 0$ and $f \in L\infty(0, T; L^2(\Omega))$, and set U_h^n be the solution of (13) with $f_h = P_h f$. If $\int_0^t (t_n - s)^{\alpha-1} \|f'(s)\| ds < \infty$ with $t > 0$, then we have

$$\| U_h^n - u(t_n) \| \le c \left(\tau t_n^{\alpha-1} \|f(0)\| + \tau \int_0^{t_n} (t_n - s)^{\alpha-1} \|f'(s)\| ds + h^2 t_n^\gamma \|f\|_{L^\infty(0,T;L^2(\Omega))} \right).$$

Proof. It suffices to bound $\| U_h^n - u_h(t_n) \|$. From (11) and (12), we have

$$U_h^n - u_h(t_n) = (F(\partial_\tau) - F(\partial_t)) f_h,$$

where $F(z) = \hat{E}_h(z)$.

By the Taylor expansion $f_h(t) = f_h(0) + 1 * f_h'$, we have

$$U_h^n - u_h(t_n) = (K(\partial_\tau) - K(\partial_t)) f_h(0) + ((K(\partial_\tau) - K(\partial_t))\, 1) * f_h' = I + II.$$

For the first term I, noting that $\| F(z) \| \le c|h(z)|$, we apply Lemma 2.2 and Lemma 2.1 (with $\sigma = 1$, $p = 1$, and some suitable parameters λ) to derive that

$$\begin{aligned} \|I\| &= \| (K(\partial_\tau) - K(\partial_t)) f_h(0) \| \\ &\le c\tau \min\left\{1, t_n^{\alpha-1}\right\} \|f_h(0)\| \le c\tau t_n^{\alpha-1} \|f(0)\|. \end{aligned}$$

The second term II has the following estimate:

$$\begin{aligned} \|II\| &\le \int_0^{t_n} \| ((K(\partial_\tau) - K(\partial_t))\, 1)(t_n - s) f_h'(s) \| ds \\ &\le c\tau \int_0^{t_n} (t_n - s)^{\alpha-1} \|f'(s)\| ds. \end{aligned}$$

Combining the above estimates I and II with Theorem 4.2, we complete the proof.

4.2.2 Error Estimate for the SBD Method

We now present the error estimates for the homogeneous problem in the next lemma.

Lemma 4.4. Let u_h and U_h^n be the solutions of Eqs. (9) and (16), respectively. Particularly, $v \in \dot{H}^2(\Omega)$, $f = 0$, and $v_h = R_h v, b_h = P_h b$. Then the following error estimates hold:

(a) If $b \in \dot{H}^2(\Omega)$ and $b_h = R_h b$, then

$$\|u_h(t_n) - U_h^n\| \le c\tau^2 \left(t_n^{\alpha-2} \|v\|_{\dot{H}^2(\Omega)} + t_n^{-1} \|b\|_{\dot{H}^2(\Omega)} \right).$$

(b) If $b \in L^2(\Omega)$ and $b_h = P_h b$, then

$$\|u_h(t_n) - U_h^n\| \le c\tau^2 \left(t_n^{\alpha-2} \|v\|_{\dot{H}^2(\Omega)} + t_n^{-1} \|b\| \right).$$

Proof. Let $F_1(z) = \hat{E}_h(z) z$ and $F_2(z) = \hat{E}_h(z) z^\alpha$. From Eqs. (14) and (15), one has

$$u_h(t_n) - U_h^n = -(F_1(\partial_t) - F_1(\partial_\tau))_{RL} D_{0,t}^{-1} (\mu A_h) v_h + (F_2(\partial_t) - F_2(\partial_\tau)) a_1 t b_h.$$

From Lemma 2.2, we have

$$\|F_1(z)\| = \|\hat{E}_h(z) z\| \le c|z| \min\left\{ |z|^{-1}, \frac{1}{a_1} |z|^{-\alpha} \right\}, \quad \forall z \in \Sigma_\theta,$$

and

$$\|F_2(z)\| = \|\hat{E}_h(z) z^\alpha\| \le c|z|^\alpha \min\left\{ |z|^{-1}, \frac{1}{a_1} |z|^{-\alpha} \right\}, \quad \forall z \in \Sigma_\theta.$$

So for the case $b \in L^2$ and $b_h = P_h b$, by Lemma 2.1 (with $\sigma = 2, p = 2$, and the suitable chosen parameters λ), we derive that

$$\begin{aligned}\|u_h(t_n) - U_h^n\| &\le \| - (F_1(\partial_t) - F_1(\partial_\tau))_{RL} D_{0,t}^{-1}(\mu A_h) v_h\| + \|(F_2(\partial_t) - F_2(\partial_\tau)) a_1 t b_h\| \\ &\le c\tau^2 \left(\min\left\{t_n^{-1}, t_n^{\alpha-2}\right\} \|v\|_{\dot{H}^2(\Omega)} + \min\left\{t_n^{-\alpha}, t_n^{-1}\right\} \|b\|\right) \\ &\le c\tau^2 \left(t_n^{\alpha-2} \|v\|_{\dot{H}^2(\Omega)} + t_n^{-1} \|b\|\right),\end{aligned}$$

The error estimates for the case $b \in \dot{H}^2(\Omega)$ and $b_h = R_h v$ is similar with that in (b), so the proof is completed.

Remark 4.4. It seems that the error estimates for the smooth data b in $\dot{H}^2(\Omega)$ in the proof of Lemma 4.4 may not be sharp due to the appearance of the prefactor t_n^{-1} in $\|b\|_{\dot{H}^2(\Omega)}$. Nevertheless, this is enough for the analysis and use of our schemes in this paper. See Remark 4.2 for some similar discussions.

Remark 4.5. Similar to the discussion of Remark 4.3, one may obtain the improved result of Lemma 4.4 with respect to the initial data $v \in L^2(\Omega)$ and $v_h = P_h v$, that is

$$\|U_h^n - u_h(t_n)\| \le c\tau^2 \left(t_n^{\gamma-2} \|v\| + t_n^{-1} \|b\|\right).$$

It seems that the convergent order may maintain the first/second-order temporal accuracy for the semidiscrete scheme (14) by using the BE/SBD scheme, even though the initial data is nonsmooth, i.e., $v \in L^2(\Omega)$, while one need to impose the condition $a_3 = 0$ in order to obtain second-order spatial accuracy in the spatial error estimate of the semidiscrete scheme, see Remark 4.1 for more details.

Now we summarize the error estimates of the SBD scheme (16) for the homogeneous problem.

Theorem 4.5. Let u and U_h^n be the solutions of (1) with $v \in \dot{H}^2(\Omega), b \in L^2(\Omega), f = 0$, and (16) with $v_h = R_h v$, respectively. Then the following error estimates holds:

(a) If $b \in \dot{H}^2(\Omega)$ and $b_h = R_h b$, then

$$\|U_h^n - u(t_n)\| \le c\left(h^2 + \tau^2 t_n^{\alpha-2}\right) \|v\|_{\dot{H}^2(\Omega)} + c\left(h^2 t_n + \tau^2 t_n^{-1}\right) \|b\|_{\dot{H}^2(\Omega)}.$$

(b) If $b \in L^2(\Omega)$, and $b_h = P_h b$, then

$$\|U_h^n - u(t_n)\| \le c\left(h^2 + \tau^2 t_n^{\alpha-2}\right) \|v\|_{\dot{H}^2(\Omega)} + c\left(h^2 t_n^{\gamma-\alpha+1} + \tau^2 t_n^{-1}\right) \|b\|.$$

Finally, we present the following error estimate for the inhomogeneous problem with $v = b = 0$.

Theorem 4.6. Let u be the solution of the problem (1) with $v = b = 0$ and $f \in L\infty(0, T; L^2(\Omega))$, and let U_h^n be the solution of (16) with $v_h = b_h = 0$. If $\int_0^t (t-s)^{\alpha-1} \|f''(s)\| ds < \infty$ for $t > 0$, then we have

$$\begin{aligned}\|u(t_n) - U_h^n\| \le c(h^2 t_n^{\gamma} \|f\|_{L^\infty(0,T;L^2(\Omega))} + \tau^2 t_n^{\alpha-2} \|f(0)\| \\ + \tau^2 t_n^{\alpha-1} \|f'(0)\| + \tau^2 \int_0^{t_n} (t_n - s)^{\alpha-1} \|f''(s)\| ds)).\end{aligned}$$

Proof. Similar to the proof of Theorem 4.4, we just need to bound $e_h^n = u_h(t_n) - U_h^n$. Using the Taylor expansion of $f_h(t)$ at $t=0$: $f_h(t) = f_h(0) + tf'_h(0) + t * f''_h$, we rewrite the expressions of $u_h(t_n)$ and U_h^n in (14) and (15) respectively as

$$u_h(t_n) = F(\partial_t)\left(\partial_{tRL} D_{0,t}^{-1} f_h(0) + tf'_h(0) + t * f''_h\right),$$

$$U_h^n = F(\partial_\tau)\left(\partial_{\tau RL} D_{0,t}^{-1} f_h(0) + tf'_h(0) + t * f''_h\right),$$

where $F(z) = \hat{E}_h(z)$. So,

$$\begin{aligned}\|e_h^n\| &\le \|\left(F(\partial_t)\,\partial_t - F(\partial_\tau)\,\partial_\tau\right)_{RL} D_{0,t}^{-1} f_h(0)\| \\ &\quad + \|\left(F(\partial_t) - F(\partial_\tau)\right) t'_h(0)\| + \|\left(\left(F(\partial_t) - F(\partial_\tau)\right) t\right) * f''_h)\| \\ &:= I + II + III.\end{aligned}$$

Noting that for $\forall z \in \Sigma_\theta$, one has

$$\|F(z)\,z\| = \|\hat{E}_h(z)\,z\| \le c|z| \min\left\{|z|^{-1}, \frac{1}{a_1}|z|^{-\alpha}\right\},$$

and

$$\|F(z)\| = \|\hat{E}_h(z)\| \le c \min\left\{|z|^{-1}, \frac{1}{a_1}|z|^{-\alpha}\right\}.$$

So for the first two terms I and II, by Lemma 2.1 (with $\sigma = 2, p = 2$, and the suitable chosen parameters λ), we obtain

$$\begin{aligned}\|I + II\| &\le c\tau^2\left(\min\left\{t_n^{-1}, t_n^{\alpha-2}\right\}\|f(0)\| + \min\left\{1, t_n^{\alpha-1}\right\}\|f'(0)\|\right) \\ &\le c\tau^2\left(t_n^{\alpha-2}\|f(0)\| + t_n^{\alpha-1}\|f'(0)\|\right).\end{aligned}$$

For the third term III, we similarly have

$$\begin{aligned}\|III\| &\le \int_0^{t_n} \|\left(\left(F(\partial_t) - F(\partial_\tau)\right) t\right)(t-s) f_{h''}(s))\| ds \\ &\le c\tau^2 \int_0^{t_n} (t_n - s)^{\alpha-1}\|f''(s)\| ds.\end{aligned}$$

Putting the bounds together we thus finish the proof.

5 Numerical Experiments

In this part, we demonstrate numerical examples to verify the theoretical results derived in previous section. In all numerical tests, we fix coefficient $\mu = a_1 = a_3 = 1$, unless otherwise specified. The spatial and temporal convergence rates are computed separately on the domain $\Omega = (0,1)^2$ and at a fixed final time T. The L^2-norm errors are measured by $\|U_h^n - u_h(t_n)\|_{L^2(\Omega)}$ at $t_n = T$.

Example 5.1. (The solution is known). Consider problem (1) with the following source term:

$f = \sin(\pi x)\sin(\pi y)(pt^{p-1} + 2\pi^2(1+t^p) + g(p,\alpha) + 2\pi^2 g(p,\gamma))$

where $g(x,y) = \frac{\Gamma(1+x)}{\Gamma(1+x-y)} t^{x-y}$.

The corresponding solution to (1) is $u(x,t) = \sin(\pi x)\sin(\pi y)(1+t^p)$. Taking $p = 2.5$ and $T = 1$, we compute the numerical solution of (1) by using the BE (13) and SBD scheme (16), respectively. The convergence rate $O(\tau^2 + h^2)$ in the L^2-norm can be observed from the numerical results in Tabs. 1 and 2, which are in line with the theoretical results.

Example 5.2. (The solution is unknown). Consider the problem (1) with the following data:

(a) $v = x(1-x)y(1-y), b = 0,$ and $f = 0,$

(b) $v = 0, b = x(1-x)y(1-y),$ and $f = 0,$

(c) $v = 0, b = \chi_{[0,1/2)\times(0,1)}(x,y),$ and $f = 0,$

(d) $v = 0,\ b = 0,$ and $f = (1+t^{1.2})\chi_{(0,1/2]\times(0,1)}(x,y).$

(e) $v = \chi_{[0,1/2)\times(0,1)}(x,y), b = 0,$ and $f = 0.$

We compute a reference solution in each case on very refined mesh due to the exact solutions of (1) with the above data are difficult to obtain. The numerical results for cases (a)–(d) with $T = 0.1$ are demonstrated on Tabs. 3–6, respectively. We observe the $O(\tau)$ and $O(\tau^2)$ rates for the temporal error for the BE and SBD schemes of (1), respectively. These observations agree well with the convergence theory.

Table 1: The L^2 norm errors in time for Example 5.1 with $h = 1/512$

Scheme	N	$(\alpha,\gamma) = (1.9, 0.8)$		$(\alpha,\gamma) = (1.5, 0.4)$		$(\alpha,\gamma) = (1.2, 0.1)$	
		L^2 error	Rate	L^2 error	Rate	L^2 error	Rate
BE	4	8.98E-02	–	4.63E-02	–	1.95E-02	–
	8	4.57E-02	0.97	2.35E-02	0.98	9.94E-03	0.97
	16	2.31E-02	0.99	1.19E-02	0.99	5.01E-03	0.99
	32	1.16E-02	0.99	5.95E-03	1.00	2.51E-03	1.00
SBD	4	1.61E-02	–	8.32E-03	–	2.83E-03	–
	8	4.07E-03	1.99	2.13E-03	1.97	7.08E-04	2.00
	16	1.00E-03	2.02	5.34E-04	2.00	1.74E-04	2.03
	32	2.42E-04	2.05	1.29E-04	2.05	3.87E-05	2.16

We also numerically examine the errors for the nonsmooth initial data $v \in L^2(\Omega)$ by using the BE and SBD schemes for (1), in which the error estimates are not available in this paper, see Tabs. 7 and 8. We observe that the temporal ones are $O(\tau)$ and $O(\tau^2)$ with three different combination of α and γ, which verify the discussions in Remarks 4.3 and 4.5. From Tab. 8, one can see that the spatial errors are affected by the parameter a_3. The smaller value of a_3, the smaller the spatial errors. This further numerically confirms the conclusion in Remark 4.1.

Table 2: The L^2 norm errors in space for Example 5.1 with $N = T/2048$

Scheme	$1/h$	$(\alpha,\gamma)=(1.9,0.8)$		$(\alpha,\gamma)=(1.5,0.4)$		$(\alpha,\gamma)=(1.2,0.1)$	
		L^2 error	Rate	L^2 error	Rate	L^2 error	Rate
	4	1.19E-01	–	1.16E-01	–	1.13E-01	–
BE	8	3.09E-02	1.94	3.01E-02	1.94	2.94E-02	1.95
	16	7.68E-03	2.01	7.52E-03	2.00	7.38E-03	1.99
	32	1.80E-03	2.09	1.82E-03	2.05	1.82E-03	2.02
	4	1.19E-01	–	1.16E-01	–	1.13E-01	–
SBD	8	3.11E-02	1.94	3.01E-02	1.94	2.94E-02	1.94
	16	7.85E-03	1.98	7.61E-03	1.99	7.41E-03	1.99
	32	1.96E-03	2.00	1.90E-03	2.00	1.85E-03	2.00

Table 3: The L^2 norm errors in time for case (a) in Example 5.2 with $h = 1/10$

Scheme	N	$(\alpha,\gamma)=(1.9,0.8)$		$(\alpha,\gamma)=(1.5,0.4)$		$(\alpha,\gamma)=(1.2,0.1)$	
		L^2 error	Rate	L^2 error	Rate	L^2 error	Rate
	16	9.68E-06	–	1.45E-04	–	2.79E-04	–
BE	32	5.03E-06	0.94	7.39E-05	0.97	1.42E-04	0.97
	64	2.57E-06	0.97	3.73E-05	0.98	7.16E-05	0.99
	128	1.30E-06	0.99	1.88E-05	0.99	3.60E-05	0.99
	16	3.88E-06	–	4.02E-06	–	6.63E-06	–
SBD	32	9.72E-07	2.00	8.88E-07	2.18	1.80E-06	1.89
	64	2.43E-07	2.00	2.08E-07	2.09	4.64E-07	1.95
	128	6.07E-08	2.00	5.04E-08	2.05	1.18E-07	1.98

Table 4: The L^2 norm errors in time for case (b) in Example 5.2 with $h = 1/10$

Scheme	N	$(\alpha,\gamma)=(1.9,0.8)$		$(\alpha,\gamma)=(1.5,0.4)$		$(\alpha,\gamma)=(1.2,0.1)$	
		L^2 error	Rate	L^2 error	Rate	L^2 error	Rate
	16	4.08E-05	–	3.11E-05	–	2.13E-05	–
BE	32	2.07E-05	0.97	1.58E-05	0.98	1.08E-05	0.98
	64	1.05E-05	0.99	7.97E-06	0.99	5.43E-06	0.99
	128	5.26E-06	0.99	4.00E-06	0.99	2.73E-06	1.00
	16	1.57E-06	–	1.74E-06	–	1.21E-06	–
SBD	32	4.11E-07	1.94	4.44E-07	1.97	3.06E-07	1.98
	64	1.05E-07	1.97	1.12E-07	1.99	7.67E-08	1.99
	128	2.63E-08	1.99	2.80E-08	2.00	1.92E-08	2.00

Table 5: The L^2 norm errors in time for case (c) in Example 5.2 with $h = 1/10$

Scheme	N	$(\alpha, \gamma) = (1.9, 0.8)$		$(\alpha, \gamma) = (1.5, 0.4)$		$(\alpha, \gamma) = (1.2, 0.1)$	
		L^2error	Rate	L^2 error	Rate	L^2 error	Rate
BE	16	5.00E-04	–	3.80E-04	–	2.60E-04	–
	32	2.54E-04	0.98	1.93E-04	0.98	1.32E-04	0.98
	64	1.28E-04	0.99	9.72E-05	0.99	6.62E-05	0.99
	128	6.43E-05	0.99	4.88E-05	0.99	3.32E-05	1.00
SBD	16	3.02E-05	–	2.71E-05	–	1.73E-05	–
	32	7.35E-06	2.04	6.59E-06	2.04	4.24E-06	2.03
	64	1.82E-06	2.02	1.63E-06	2.02	1.05E-06	2.01
	128	4.51E-07	2.01	4.05E-07	2.01	2.61E-07	2.01

Table 6: The L^2 norm errors in time for case (d) in Example 5.2 with $h = 1/10$

Scheme	N	$(\alpha, \gamma) = (1.9, 0.8)$		$(\alpha, \gamma) = (1.5, 0.4)$		$(\alpha, \gamma) = (1.2, 0.1)$	
		L^2 error	Rate	L^2 error	Rate	L^2 error	Rate
BE	16	1.51E-05	–	9.13E-05	–	1.65E-04	–
	32	7.77E-06	0.96	4.65E-05	0.97	8.35E-05	0.98
	64	3.95E-06	0.98	2.35E-05	0.99	4.21E-05	0.99
	128	1.99E-06	0.99	1.18E-05	0.99	2.11E-05	0.99
SBD	16	2.13E-06	–	4.11E-06	–	7.55E-06	–
	32	5.30E-07	2.00	9.87E-07	2.06	1.84E-06	2.04
	64	1.32E-07	2.00	2.42E-07	2.03	4.55E-07	2.01
	128	3.29E-08	2.00	5.98E-08	2.01	1.13E-07	2.01

Table 7: The L^2 norm errors in time for case (e) in Example 5.2 with $h = 1/10$

Scheme	N	$(\alpha, \gamma) = (1.9, 0.8)$		$(\alpha, \gamma) = (1.5, 0.4)$		$(\alpha, \gamma) = (1.2, 0.1)$	
		L^2 error	Rate	L^2 error	Rate	L^2 error	Rate
BE	16	8.25E-04	–	3.17E-03	–	4.03E-03	–
	32	4.22E-04	0.97	1.60E-03	0.98	2.02E-03	1.00
	64	2.14E-04	0.98	8.05E-04	0.99	1.01E-03	1.00
	128	1.07E-04	0.99	4.04E-04	1.00	5.07E-04	1.00
SBD	16	5.30E-05	–	1.95E-04	–	3.49E-04	–
	32	1.29E-05	2.04	4.79E-05	2.03	8.19E-05	2.09
	64	3.18E-06	2.02	1.19E-05	2.02	1.99E-05	2.04
	128	7.91E-07	2.01	2.95E-06	2.01	4.91E-06	2.02

Table 8: The L^2 norm errors in space for case (e) in Example 5.2 with $N = 100$, $\alpha = 1.5$, and $\gamma = 0.4$

Scheme	$1/h$	$a_3 = 1$		$a_3 = 0.01$		$a_3 = 1E-8$	
		L^2 error	Rate	L^2 error	Rate	L^2 error	Rate
BE	8	8.18E-02	–	1.97E-02	–	2.16E-02	–
	16	5.71E-02	0.52	6.64E-03	1.57	7.03E-03	1.62
	32	4.02E-02	0.51	2.00E-03	1.73	1.89E-03	1.90
	64	2.84E-02	0.50	8.27E-04	1.27	4.76E-04	1.99
SBD	8	8.18E-02	–	2.04E-02	–	2.24E-02	–
	16	5.71E-02	0.52	7.00E-03	1.54	7.45E-03	1.59
	32	4.02E-02	0.51	2.09E-03	1.74	2.02E-03	1.88
	64	2.84E-02	0.50	8.40E-04	1.32	5.10E-04	1.98

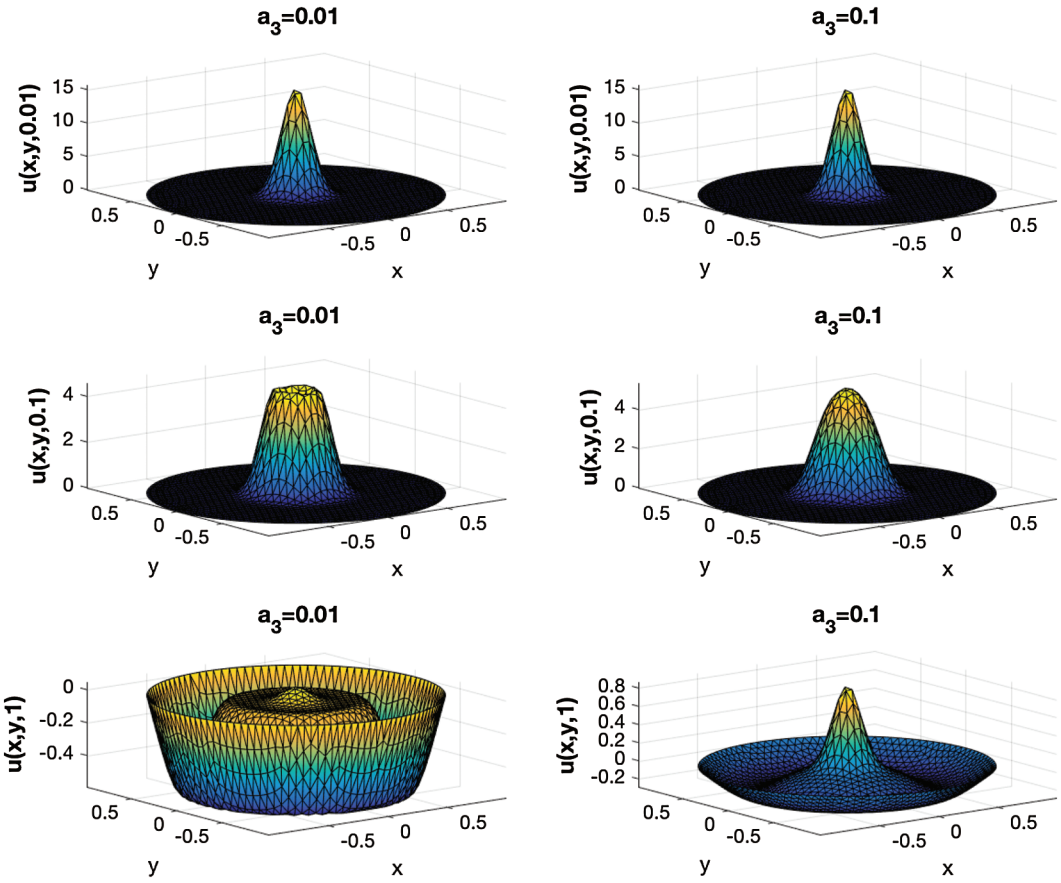

Figure 1: Comparison behavior of $u(x, y, 0.01), u(x, y, 0.1)$ and $u(x, y, 1)$ for (1) with fixed $(\alpha, \gamma) = (1.9, 0.5)$ and different a_3, computed by SBD scheme with $h = 0.05$, $N = 200$

Example 5.3. In this example, we perform numerical simulation on the model (1) with the following data: $f=0, b=0$, and

$$v=\frac{1}{2\pi\sigma^2}\exp\left(-\frac{x^2+y^2}{2\sigma^2}\right),$$

with the parameter σ denotes the impact level of the initial values. Here, we let $\sigma=0.1$.

The computational domain is on a circle $\Omega=(x,y)|x^2+y^2=1$, in which we are more interested. The numerical results are demonstrated in Fig. 1.

For fixed $a_3=0.01$ in Fig. 1, the peak of the solution is located at the origin at the beginning. However as time goes by, say, $t=0.1$, the peak of the solution to the Eq. (1) is no longer at the origin, but spreads around the origin. This phenomenon becomes more apparent with increasing time and exhibits a period-like evolution. Compared to the case $a_3=0.01$, the evolution of the solution in case $a_3=0.1$ becomes slower, see the right-hand column in Fig. 1 for the details. From Fig. 1, we can also observe that the solution of the model is not significantly different for various parameters $a_3=0.01$ and 0.1 at the beginning $t=0.01$. As time goes by, the effect of the value of parameter a_3 on the model becomes more and more obvious. It seems that the smaller the parameter a_3, the more the fractional model (1) behaves like the time-fractional diffusion-wave equation with damping [13]. This may further validates the claims in [9] that the fractional derivative acting on the Laplacian in the model (1) may be used to capture the viscoelastic behavior of the flow.

6 Conclusions

In this paper we have proposed two efficient and robust fully discrete schemes for the time-fractional Oldroyd-B fluid equation which involves the Caputo derivative in time. These two numerical schemes are based on Galerkin finite element method in space and convolution quadrature in time. The error estimates for the schemes are investigated with respect to data regularity. Numerical results are provided and they are all well agree with the theoretical results.

We find that the spatial errors of the proposed schemes would be deteriorated if the data $v\in L^2(\Omega)$ due to the appearance of the term ${}_CD_{0,t}^{\gamma}$ acting on the Laplacian in (1), while the temporal errors are not affected. It seems that such situation does not exist in other similar fractional model which involves the R–L derivative in time [9,10]. So this makes the numerical investigation of fractional model considered in this paper more difficult. Nevertheless, we make some comments on such situation and numerically confirm our conclusions, see Remarks 4.1, 4.3, and 4.5, and Tabs. 7 and 8.

Our strategy in this paper can be extended to solve other types of fractional models, for example, the non-Newtonian fluid model [2]

$$\left(\partial_t+a_1{}_CD_{0,t}^{\alpha}\right)u(x,t)+\kappa\left(1+a_2{}_CD_{0,t}^{\beta}\right)u(x,t)=\mu\left(1+a_3{}_CD_{0,t}^{\gamma}\right)\Delta u(x,t)+f(x,t),$$

which can be regarded as a more general case of (1). It seems that the numerical study is trivial so we omit the details here. It is noteworthy that our numerical schemes are not very computationally efficient for long time problems due to the nonlocal nature of Caputo derivative and the high dimensionality of the space. Recently, some authors have proposed fast algorithms to resolve such issue, [23–25], just to name a few. So combining the numerical schemes here with a fast algorithm is an interesting thing to do and worthy of further study.

Acknowledgement: The author wishes to express his appreciation to the reviewers for their helpful suggestions which greatly improved the presentation of this paper.

Funding Statement: The work is supported by the Guangxi Natural Science Foundation [Grant Numbers 2018GXNSFBA281020, 2018GXNSFAA138121] and the Doctoral Starting up Foundation of Guilin University of Technology [Grant Number GLUTQD2016044].

Conflicts of Interest: The author declares that he has no conflicts of interest to report regarding the present study.

References

1. Mainardi, F. (2010). *Fractional calculus and waves in linear viscoelasticity*. London: Imperial College Press.
2. Feng, L., Liu, F., Turner, I., Zheng, L. (2018). Novel numerical analysis of multi-term time fractional viscoelastic non-Newtonian fluid models for simulating unsteady MHD Couette flow of a generalized Oldroyd-B fluid. *Fractional Calculus and Applied Analysis, 21(4),* 1073–1103. DOI 10.1515/fca-2018-0058.
3. Khan, M., Ali, S. H., Qi, H. (2009). Some accelerated flows for a generalized Oldroyd-B fluid. *Nonlinear Analysis: Real World Applications, 10(2),* 980–991. DOI 10.1016/j.nonrwa.2007.11.017.
4. Riaz, M. B., Imran, M. A., Shabbir, K. (2016). Analytic solutions of Oldroyd-B fluid with fractional derivatives in a circular duct that applies a constant couple. *Alexandria Engineering Journal, 55(4),* 3267–3275. DOI 10.1016/j.aej.2016.07.032.
5. Imran, M. A., Shah, N. A., Khan, I., Aleem, M. (2016). Applications of non-integer Caputo time fractional derivatives to natural convection flow subject to arbitrary velocity and Newtonian heating. *Neural Computing and Applications, 30(5),* 1589–1599. DOI 10.1007/s00521-016-2741-6.
6. Anwar, M. S. (2020). Numerical study of transport phenomena in a nanofluid using fractional relaxation times in Buongiorno model. *Physica Scripta, 95(3),* 035211. DOI 10.1088/1402-4896/ab4ba9.
7. Li, C., Zeng, F. (2015). *Numerical methods for fractional calculus*. Boca Raton: Chapman and Hall/CRC.
8. Zhang, J., Liu, F., Anh, V. V. (2019). Analytical and numerical solutions of a two-dimensional multi-term time-fractional Oldroyd-B model. *Numerical Methods for Partial Differential Equations, 35(3),* 875–893. DOI 10.1002/num.22327.
9. Bazhlekova, E., Jin, B., Lazarov, R., Zhou, Z. (2015). An analysis of the Rayleigh–Stokes problem for a generalized second-grade fluid. *Numerische Mathematik, 131(1),* 1–31. DOI 10.1007/s00211-014-0685-2.
10. Al-Maskari, M., Karaa, S. (2019). Galerkin FEM for a time-fractional Oldroyd-B fluid problem. *Advances in Computational Mathematics, 45(2),* 1005–1029. DOI 10.1007/s10444-018-9649-x.
11. Ren, J., Gao, G. H. (2014). Efficient and stable numerical methods for the two-dimensional fractional Cattaneo equation. *Numerical Algorithms, 69(4),* 795–818. DOI 10.1007/s11075-014-9926-9.
12. Zhao, X., Sun, Z. Z. (2014). Compact Crank–Nicolson schemes for a class of fractional Cattaneo equation in Inhomogeneous medium. *Journal of Scientific Computing, 62(3),* 747–771. DOI 10.1007/s10915-014-9874-5.
13. Chen, A., Li, C. (2017). An alternating direction Galerkin method for a time-fractional partial differential equation with damping in two space dimensions. *Advances in Difference Equations, 2017(1),* 1–17. DOI 10.1186/s13662-016-1057-2.
14. Li, H., Jiang, W., Li, W. (2019). Space-time spectral method for the cattaneo equation with time fractional derivative. *Applied Mathematics and Computation, 349,* 325–336. DOI 10.1016/j.amc.2018.12.050.
15. Ji, C. C, Dai, W., Sun, Z. Z (2019). Numerical schemes for solving the time-fractional dual-phase-lagging heat conduction model in a double-layered nanoscale thin film. *Journal of Scientific Computing, 81(3),* 1767–1800. DOI 10.1007/s10915-019-01062-6.

16. Jin, B., Li, B., Zhou, Z. (2017). Correction of high-order BDF convolution quadrature for fractional evolution equations. *SIAM Journal on Scientific Computing, 39(6),* A3129–A3152. DOI 10.1137/17M1118816.
17. Guo, L., Zeng, F., Turner, I., Burrage, K., Karniadakis, G. E. (2019). Efficient multistep methods for tempered fractional calculus: algorithms and simulations. *SIAM Journal on Scientific Computing, 41(4),* A2510–A2535. DOI 10.1137/18M1230153.
18. Lubich, C. (1988). Convolution quadrature and discretized operational calculus. I. *BIT Numerical Mathematics, 52(2),* 129–145. DOI 10.1007/BF01398686.
19. Jin, B., Lazarov, R., Zhou, Z. (2016). Two fully discrete schemes for fractional diffusion and diffusion-wave equations with nonsmooth data. *SIAM Journal on Scientific Computing, 38(1),* A146–A170. DOI 10.1137/140979563.
20. Thomée, V. (2006). *Galerkin finite element methods for parabolic problems*. 2nd edition. Berlin: Springer.
21. Cuesta, E., Lubich, C., Palencia, C. (2006). Convolution quadrature time discretization of fractional diffusion-wave equations. *Mathematics of Computation, 75(254),* 673–696. DOI 10.1090/S0025-5718-06-01788-1.
22. Lubich, C. (2004). Convolution quadrature revisited. *BIT Numerical Mathematics, 44(3),* 503–514. DOI 10.1023/B:BITN.0000046813.23911.2d.
23. Zeng, F., Turner, I., Burrage, K. (2018). A stable fast time-stepping method for fractional integral and derivative operators. *Journal of Scientific Computing, 77(1),* 283–307. DOI 10.1007/s10915-018-0707-9.
24. Zhu, H., Xu, C. (2019). A fast high order method for the time-fractional diffusion equation. *SIAM Journal on Numerical Analysis, 57(6),* 2829–2849. DOI 10.1137/18M1231225.
25. Jin, B., Zhou, Z. (2020). Incomplete iterative solution of subdiffusion. *Numerische Mathematik, 145(3),* 693–725. DOI 10.1007/s00211-020-01128-w.